Journal of Cardiology 61 (2013) 354–358

Journal of Cardiology
journal homepage: www.elsevier.com/locate/jjcc

Original article

How is the peri-patch myocardium in ventricular septal defect patch repair?

Lucy Youngmin Eun (MD)[a], Han Ki Park (MD)[b], Jae Young Choi (MD)[a,*]

[a] Division of Pediatric Cardiology, Department of Pediatrics, Yonsei University College of Medicine, Seoul, Republic of Korea
[b] Division of Cardiovascular Surgery, Department of Thoracic Surgery, Yonsei University College of Medicine, Seoul, Republic of Korea

ARTICLE INFO

Article history:
Received 20 June 2012
Received in revised form
18 November 2012
Accepted 22 December 2012
Available online 21 March 2013

Keywords:
Tissue Doppler echocardiography
Strain
Peri-patch region
Myocardial function

ABSTRACT

Strain rate (SR) and strain (ε) in tissue Doppler imaging provide new noninvasive measurements of myocardial function, independent of heart motion.
This study assesses the extent of peri-patch regional myocardial function after patch repair of ventricular septal defect (VSD).
Myocardial SR and ε were recorded from the peri-patch myocardium and remote septum from patch area in 18 patients (1 month to 4 years of age, mean 2.3 years). Distance between the patch and the point of returning to remote normal strain (ε) profile was measured.
Compared to the remote myocardial region, peri-patch myocardium had decreased peak longitudinal SR ($-3.8 \pm 2.1\ s^{-1}$ vs. $-5.3 \pm 3.3\ s^{-1}$, $p < 0.05$), delayed time to peak longitudinal SR (144 ± 59 ms vs. 110 ± 46 ms, $p < 0.05$), decreased peak ε (longitudinal, -20.8 ± 8.1% vs. -28.7 ± 11.1%; radial, 20.1 ± 16.3% vs. 34.3 ± 22.4%, $p < 0.01$), and delayed time to peak ε (longitudinal, 314 ± 80 ms vs. 241 ± 63 ms; radial, 329 ± 99 ms vs. 265 ± 78 ms, $p < 0.0001$).
The mean distance from the patch to the remote patch ε curve was 2.55 ± 0.77 mm.
Conclusion: Peri-patch myocardium after repair of VSD has delayed and diminished contraction as compared to more remote normal myocardium.

Introduction

Non-invasive assessment of ventricular function in children could benefit from a technique that would characterize local myocardial deformation [1–6].

Myocardial wall velocities using tissue Doppler have been proposed as an advanced non-invasive modality of quantifying regional myocardial function in children [1–9]. However, tissue Doppler myocardial imaging detects regional velocity profiles with respect to the position of the transducer. Such velocities may be affected by cardiac movement and motion by contraction in adjacent myocardial segments [10].

In order to surmount this problem, techniques have become available to calculate local strain rate (SR) and strain (ε) from measured local spatial gradients in myocardial wall velocities [6,11]. These two parameters are able to characterize regional deformation of local myocardium. Peak SR represents the maximal velocity of deformation during systole, and regional systolic strain represents the magnitude of myocardial deformation from a reference point [11].

In adult patients, regional SR and ε calculation have been shown to quantify regional myocardial function in ischemic myocardium and after myocardial infarction [12–14]. In healthy children 4–16 years of age, normal systolic and diastolic longitudinal SR and ε values from all segments of the left and right ventricles have been defined [1,6,15,16].

SR and ε have been demonstrated to be homogenous along the extent of the ventricular septum. The effect of open heart surgery in congenital heart disease may have a detrimental effect on regional myocardial function, but this has not been systematically explored. Understanding the long- and short-term effects of myocardial injury by sewing or patch placement could potentially facilitate improved surgical techniques.

The purpose of this study was to quantify regional myocardial function near the ventricular septal patch in repaired ventricular septal defect (VSD) patients. Myocardial function of the peri-patch region was compared to the remote septal region which was assumed to provide a reference value.

Hypothesis

1. Normal SR and ε may be demonstrated at the remote septum far from the patch.
2. The systolic SR and ε values may be different at the peri-patch when compared to the remote myocardium.

* Corresponding author at: Division of Pediatric Cardiology, Severance Cardiovascular Hospital, Yonsei University College of Medicine 50 Yonsei-ro, Seodaemun-gu, Seoul 120-752, Republic of Korea. Tel.: +82 2 2228 8473; fax: +82 2 312 9538.
E-mail address: cjy0122@yuhs.ac (J.Y. Choi).

0914-5087/$ – see front matter © 2013 Japanese College of Cardiology. Published by Elsevier Ltd. All rights reserved.
http://dx.doi.org/10.1016/j.jjcc.2012.12.016

3. The time to peak ε may be different at the peri-patch from the remote myocardium.

Methods

Color tissue Doppler imaging (TDI) was recorded from parasternal long- and short-axis, and apical views in 18 patients (1 month to 4 years of age, mean 2.3 years of age), at the time of 1 month to 2 years after patch repair of VSD. Color TDI-derived spectral tracings of SR and ε were recorded from the peri-patch region, and from the remote septum of half distance between patch and apex. Peak values and time to peak values were compared between peri-patch and remote sites during systole and diastole. The mean distance between the patch and the point of returning to remote ε profile was measured.

Patient population

Eighteen patients with ages ranging from 1 month to 4 years (mean 2.3 years) were studied within 1 month to 2 years after patch repair of VSD. The perimembranous type and the muscular type of VSDs were included in this study. The sizes of the defect were 5–9 mm.

Definition

The two areas of myocardium immediately adjacent to each side of the patch were defined as the peri-patch area.

The segments of the septum far from the patch but adjacent to the peri-patch area were defined to be the remote-patch area.

Echocardiography

Echocardiographic studies were performed with the use of a Vingmed System V GE® (Horten, Norway) echocardiographic machine. Color TDI data were obtained in fundamental mode (2.5 MHz transducer) during three consecutive heart cycles. The digital data were recorded from the left ventricle and ventricular septum including patch, using standard and modified parasternal long-axis view, short-axis view, and apical four-chamber view.

Off-line analysis

Color tissue Doppler myocardial imaging was stored in digital format and transferred to a computer workstation for off-line analysis using EchoPac® software (GE Medical Systems, Milwaukee, WI, USA).

Longitudinal regional myocardial flow velocities were taken from color flow Doppler tissue loops from the apical views. Radial regional myocardial flow velocities were recorded from parasternal views. Color tissue Doppler myocardial imaging-derived spectral tracings of SR and ε were calculated and recorded from the peri-patch region, and from the remote septum half distance between patch and apex.

The distance between two points for measurements of myocardial deformation was set at 0.4–0.6 cm by EchoPac® software in this study. These distances were chosen in consideration of spatial sensitivity, although a distance between 0.5 cm and 1.0 cm has been frequently used in adults [7]. Peak values and time to peak values were compared between peri-patch and remote myocardium during systole and diastole. Finally, the distance between the patch and return to remote ε profile was measured by progressively moving the sample site toward apex away from the patch until ε profile became subjectively similar to the remote profile (Figs. 1–3).

Results

SR and ε of the remote myocardium

Because of lack of established normal values for SR and ε of the ventricular septum in this age group, the remote values were used as the patient's intrinsic reference values for comparison. The peak value of longitudinal systolic SR, magnitude of peak longitudinal ε were greater in magnitude and more variable than normal values for the mid septum in 4–16 year olds reported by Sutherland's group [16] (Table 1; Fig. 4). ε values are less variable and are closer to the published longitudinal normal values for 4–16 year old

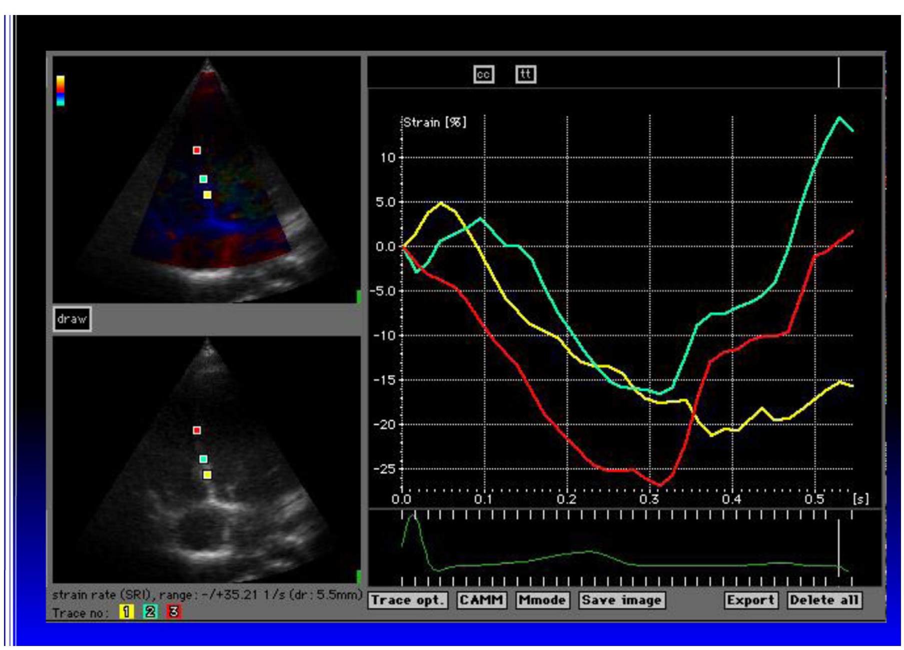

Fig. 1. Longitudinal strain at the middle of the patch, and at the point from peri-patch to remote myocardium. Yellow, patch; green, peri-patch; red, remote myocardium. (For interpretation of the references to color in this figure legend, the reader is referred to the web version of this article.)

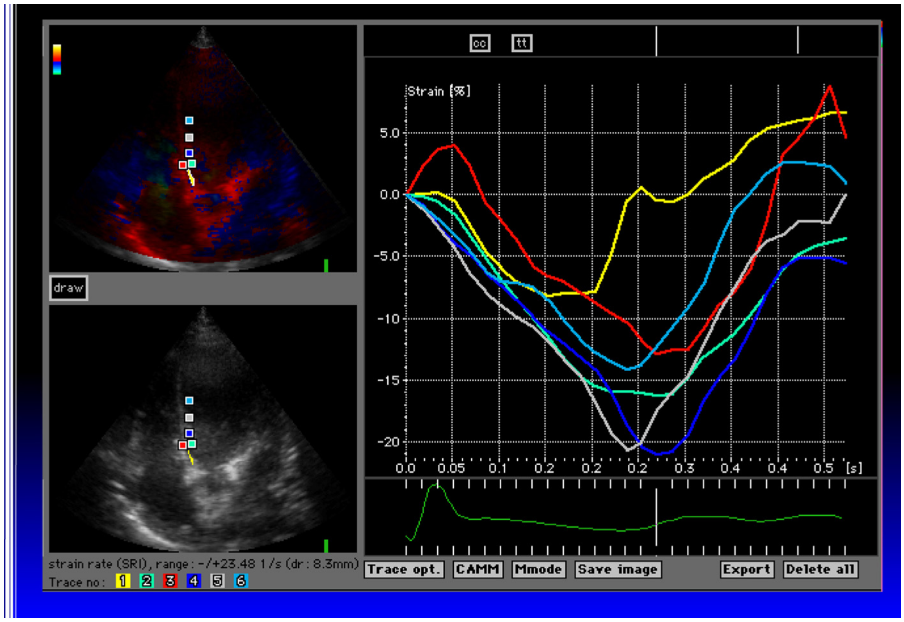

Fig. 2. Longitudinal strain at the point from peri-patch to remote myocardium. Yellow, patch; red, peri-patch; dark blue, remote myocardium. (For interpretation of the references to color in this figure legend, the reader is referred to the web version of this article.)

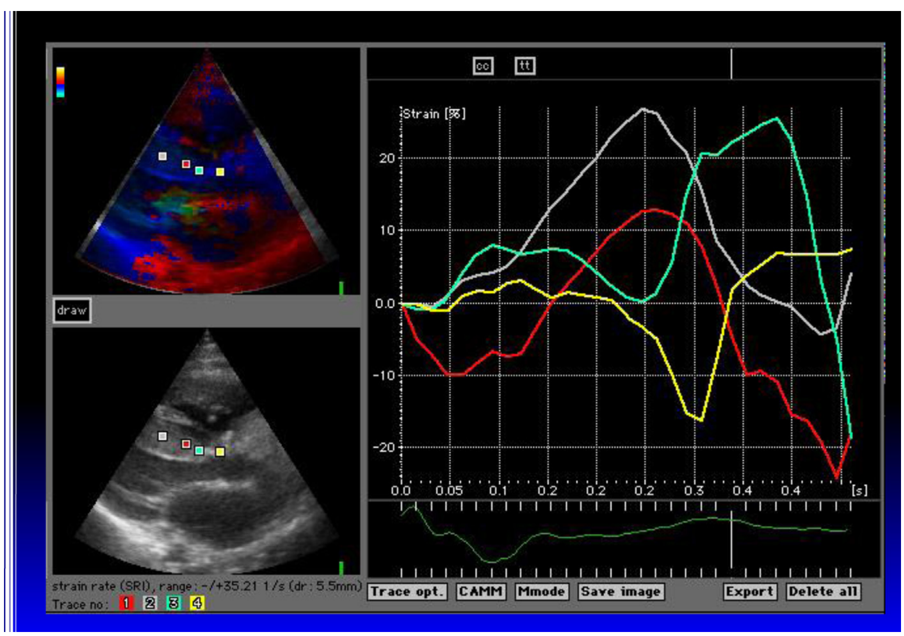

Fig. 3. Radial strain at the point from peri-patch to remote myocardium. Yellow, patch; red, peri-patch; dark blue, remote myocardium. (For interpretation of the references to color in this figure legend, the reader is referred to the web version of this article.)

Table 1
Systolic and diastolic strain rate (unit: s^{-1}) and systolic strain (unit: %) for peri-patch and remote ventricular septal longitudinal and radial function.

	Strain rate			Strain
	Systolic	Early diastolic	Late diastolic	Systolic
Longitudinal				
Peri-patch septum	−3.8 ± 3.1	4.1 ± 1.6	4.0 ± 2.3	−20.8 ± 8.1
Remote septum	−5.3 ± 4.1*	5.6 ± 3.5*	3.4 ± 1.9	−28.7 ± 11.1*
Radial				
Peri-patch septum	3.3 ± 1.8	−4.0 ± 3.1	−3.6 ± 3.4	20.1 ± 16.3
Remote septum	3.8 ± 1.6	−7.0 ± 3.1*	−5.7 ± 5.5*	34.3 ± 22.4*

* $p < 0.05$.

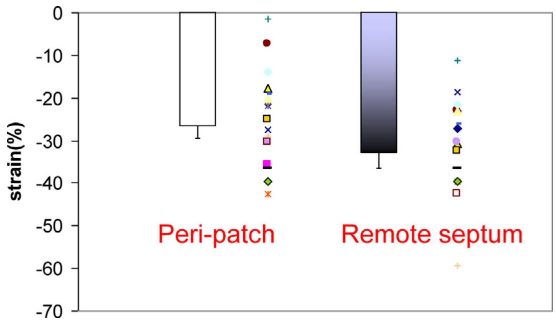

Fig. 4. Longitudinal systolic strain (%) at peri-patch and remote septal region in 18 patients.

children [16]. Normal values of septal radial strain were not available for comparison until now.

SR and ε of the peri-patch region

When compared to the more remote myocardium, the peri-patch region had decreased peak longitudinal SR (peri-patch: $-3.8 \pm 2.1\,s^{-1}$; remote: $-5.3 \pm 3.3\,s^{-1}$, $p < 0.05$), delayed time to peak systolic longitudinal SR (peri-patch: 144 ± 59 ms; remote: 110 ± 46 ms, $p < 0.01$), decreased peak ε (longitudinal, peri-patch: $-20.8 \pm 8.1\%$, remote: $-28.7 \pm 11.1\%$, $p < 0.01$; radial, peri-patch: $20.1 \pm 16.3\%$, remote: $34.3 \pm 22.4\%$, $p < 0.0001$), and delayed time to peak ε (longitudinal, peri-patch: 314 ± 80 ms, remote: 241 ± 63 ms; radial, peri-patch: 329 ± 99 ms, remote: 265 ± 78 ms, $p < 0.0001$) (Table 2). In diastole, the peri-patch myocardium had decreased peak radial SR (peri-patch: $-4.0 \pm 3.1\,s^{-1}$, remote: $-7.0 \pm 3.1\,s^{-1}$, $p < 0.01$) and increased time to peak SR (peri-patch: 353 ± 91 ms, remote: 349 ± 109 ms) (Table 2).

Measured mean distance from patch to ε profile subjectively similar to remote spectral profile was 2.55 ± 0.77 mm, so within 2.0–3.5 mm distance from the patch, the ε parameters were demonstrated to be normal.

Discussion

Some forms of congenital heart disease are likely characterized by regional abnormalities in myocardial function. Investigation of regional myocardial function in congenital heart disease has been limited. Recently, myocardial strain parameters using tissue Doppler velocities have been explored as an effective method for regional myocardial deformation. Peak SR represents the maximal velocity of deformation during systole, and regional systolic ε value represents the magnitude of myocardial deformation from a reference point [11]. In normal myocardium of children 4–16 years of age, longitudinal myocardial fibers shorten during systole, resulting in negative SR of $-1.9 \pm 0.6\,s^{-1}$ and ε values of $-24 \pm 6\%$. Values are homogeneous from the base through the mid and apical septum [6,16]. Myocardial fiber lengthening during diastole results in positive SR and ε, in apical four-chamber view. Radial ε values measured from parasternal views demonstrate thickening during systole (positive SR and ε) and thinning during diastole (negative SR and ε).

This study investigates regional myocardial deformation adjacent to VSD patch in comparison to the more distal septal myocardium. The peak value of longitudinal systolic SR, magnitude of peak longitudinal ε were greater in magnitude and more variable than normal values for the mid septum in 4–16 year olds reported by Sutherland et al. [16] (Table 1). ε values are less variable and are closer to the published longitudinal normal values for 4–16 year old children. Interestingly, values of longitudinal SR and ε of the "normal" remote myocardium were greater and more variable than published normals for 4–16 year olds [16]. Increased variability in our study may be a result of smaller sample volume used and perhaps postoperative changes. The greater magnitude of SR and ε as compared to the published normal values may be related the younger age population studied in this investigation. The pediatric normal strain values reported by Weidemann and Sutherland's group [17] are greater in magnitude to those authors' reported adult normal values of longitudinal SR $-1.4 \pm 0.1\,s^{-1}$ by Voigt et al. [18], and ε $-19.4 \pm 3.3\%$ by Garcia's group [19] (Table 1). It is likely that this trend may continue throughout infants and younger children.

The results of this study demonstrate that the abnormalities of myocardial contraction of the peri-patch are remarkable in both longitudinal and radial direction (Table 2). It is noteworthy that, in most patients, mean values of the peri-patch region are similar and not different statistically from that of remote "normals". A small number of values are significantly different and may represent a more dramatically effected subgroup.

In this study, the myocardium adjacent to a VSD patch had decreased maximal systolic SR (contraction velocity), delayed and diminished absolute ε as compared to remote myocardium. Fortunately, in this study group of patients, abnormalities tended to be small and to normalize a short distance from the patch. However, degree of variation of SR and ε from the "normal" remote region is variable with a small proportion of patients demonstrating substantial differences. While it would be interesting to investigate the causes for the acute changes of peri-patch myocardium, this was not possible in this study due to the small patient population. A detailed investigation of peri-patch myocardial function in a large patient group may provide insights into the causes of substantial ventricular dysfunction, which occasionally occurs in some patients after VSD repair.

Myocardial regional abnormalities have been best described related to ischemic heart disease [20]. Myocardial infarction induces a delay in the onset of contraction, a progressive decrease in the rate and degree of thickening, and a progressive delay in the timing of peak thickening until this event occurs in what early diastole is for the surrounding non-ischemic myocardial segments [21,22]. It is interesting that peri-patch contraction abnormalities are similar in character, but seem to be less in degree to those of ischemic myocardium. One is tempted to surmise that impairment of perfusion related to the VSD patch and sutures likely occurs. Just as likely, scarring and fibrosis, which may only be in part perfusion-related, contribute to abnormalities in regional myocardial function. Certainly, the effect of tethering of myocardium to a paradoxically moving patch is not well understood. The mechanism of peri-patch myocardial impairment is likely myriad.

However, the difference in SR in the radial direction is most substantial. This may be partially explained by the difference of the architecture of the myocardial fibers. Although the septum consists of a mixture of longitudinal, oblique, and circular radial muscle

Table 2
Time (ms) to peak systolic and diastolic strain rate and systolic strain for peri-patch and remote ventricular septal longitudinal and radial function.

	Strain rate			Strain
	Systolic	Early diastolic	Late diastolic	Systolic
Longitudinal				
Peri-patch septum	144 ± 59	371 ± 87	497 ± 148	314 ± 80
Remote septum	110 ± 46*	357 ± 83*	486 ± 146	241 ± 63*
Radial				
Peri-patch septum	147 ± 49	353 ± 91	464 ± 136	329 ± 99
Remote septum	164 ± 20	349 ± 109	460 ± 138	265 ± 78*

* $p < 0.05$.

fibers, in diastole, the circular radial muscle fiber may be a dominant deformation component in the ventricular septum. This result is similar to the report of the compensatory augmentation of radial strain attenuation in hypertrophied hypertensive heart [23].

The duration of bypass time may influence this peri-patch myocardial deformation. Understanding the long- and short-term effects of myocardial injury by sewing method or patch placement could potentially facilitate improved surgical techniques.

In summary, the peri-patch myocardium demonstrated that not only systolic contraction is delayed and diminished to variable degrees as compared to the remote myocardium, but also diastolic relaxation was diminished and delayed in the peri-patch region.

Limitations

The lack of published normal myocardial ε values for this patient group required use of more distal, likely unaffected myocardium for "normal" comparison.

Measures of SR and ε using current technology are typically limited by image and signal quality. The SR signal tends to be noisier than ε, and the determination of peak value can be difficult [1–7,23–25]. Measures in this study used a small sample volume to identify local myocardial function and to limit the direct effect of the patch on peri-patch measures. This likely led to larger variability in measures.

Conclusions

Peri-patch myocardium after repair of VSD has delayed and diminished contraction and contraction velocity as compared to more remote myocardium. This effect seems most pronounced in the radial direction. Motion pattern returns to remote profile at a small distance beyond the patch.

The peri-patch septal myocardium contracts in a manner with lesser magnitude than that of hypokinetic myocardium of myocardial ischemia.

In the near future, the successive change of this regional myocardial function should be observed for appropriate quantitative assessment over time after patch repair operation.

References

[1] Sato Y, Maruyama A, Ichihashi K. Myocardial strain of the left ventricle in normal children. J Cardiol 2012;486:1–5.

[2] Ichihashi K, Sato A, Shiraishi H, Momoi M. Tissue Doppler combined with pulsed-wave Doppler echocardiography for evaluating ventricular diastolic function in normal children. Echocardiography 2011;28:93–6.

[3] Liang XC, Cheung EW, Wong SJ, Cheung YF. Impact of right ventricular volume overload on three-dimensional global left ventricular mechanical dyssynchrony after surgical repair of tetralogy of Fallot. Am J Cardiol 2008;102:1731–6.

[4] Cheung EW, Liang XC, Lam WW, Cheung YF. Impact of right ventricular dilation on left ventricular myocardial deformation in patients after surgical repair of tetralogy of Fallot. Am J Cardiol 2009;104:1264–70.

[5] Fernandes FP, Manlhiot C, Roche SL, Grosse-Wortmann L, Slorach C, McCrindle BW, Mertens L, Kantor PF, Friedberg MK. Impaired left ventricular myocardial mechanics and their relation to pulmonary regurgitation, right ventricular enlargement and exercise capacity in asymptomatic children after repair of tetralogy of Fallot. J Am Soc Echocardiogr 2012;25:494–503.

[6] Weidemann F, Eyskens B, Jamal F, Mertens L, Kowalski M, D'Hooge J, Bijnens B, Gewilling M, Rademakers F, Hatle L, Sutherland GR. Quantification of regional left and right ventricular radial and longitudinal function in healthy children using ultrasound-based strain rate and strain imaging. J Am Soc Echocardiogr 2002;15:20–8.

[7] Friedberg MK, Fernandes FP, Roche SL, Grosse-Wortmann L, Manlhiot C, Fackoury C, Slorach C, McCrindle BW, Mertens L, Kantor PF. Impaired right and left ventricular diastolic myocardial mechanics and filling in asymptomatic children and adolescents after repair of tetralogy of Fallot. Eur Heart J Cardiovasc Imaging 2012;13:905–13.

[8] Rychik J, Tian ZY. Quantitative assessment of myocardial tissue velocities in normal children with Doppler tissue imaging. Am J Cardiol 1996;77:1254–7.

[9] Kapusta L, Thijssen JM, Cuypers MH, Peer PG, Daniels O. Assessment of myocardial velocities in healthy children using tissue Doppler imaging. Ultrasound Med Biol 2000;26:229–37.

[10] Miyatake K, Yamagishi M, Tanaka N, Uematsu M, Yamazaki N, Mine Y. New method for evaluating left ventricular wall motion by color-coded tissue Doppler imaging: in vitro and in vivo studies. J Am Coll Cardiol 1995;25:717–24.

[11] Weidemann F, Jamal F, Sutherland GR, Claus P, Kowalski M, Hatle L, Scheerder I, Bijnens B, Rademakers FE. Myocardial function defined by strain rate and strain during alterations in inotropic states and heart rate. Am J Physiol Heart Circ Physiol 2002;283:792–9.

[12] Jamal F, Kukulski T, D'hooge J, De Scheerder I, Sutherland GR. Abnormal postsystolic thickening in acutely ischemic myocardium during coronary angioplasty: a velocity, strain, and strain rate Doppler myocardial imaging study. J Am Soc Echocardiogr 1999;12:994–6.

[13] Heimddal A, Stoylen A, Torp H, Skjaerpe T. Real time strain rate imaging of the left ventricle by ultrasound. J Am Soc Echocardiogr 1998;11:1013–9.

[14] Voigt JU, Arnold M, Karlsson M, Hubbert L, Kukulski T, Hatle L. Assessment of regional longitudinal strain rate derived from Doppler myocardial imaging indices in normal and infarcted myocardium. J Am Soc Echocardiogr 2000;13:588–98.

[15] Weidemann F, Eyskens B, Mertens L, Dommke C, Kowalski M, Simmons L, Claus P, Bijnens B, Gewillig M, Hatle L, Sutherland GR. Quantification of regional right and left ventricular function by ultrasonic strain rate and strain indexes after surgical repair of tetralogy of Fallot. Am J Cardiol 2002;90(2):133–8.

[16] Weidemann F, Eyskens B, Sutherland GR. New ultrasound methods to quantify regional myocardial function in children with heart disease. Pediatr Cardiol 2002;23:1053–64.

[17] Weidemann F, Kowalski M, D'hooge J, Bijnens B, Sutherland GR. Doppler myocardial imaging. A new tool to assess regional inhomogeneity in cardiac function. Basic Res Cardiol 2001;96:595–605.

[18] Voigt JU, Lindenmeier G, Exner B, Regenfus M, Werner D, Reulbach U, Nixdorff U, Flachskampf FA, Daniel WG. Incidence and characteristics of segmental postsystolic longitudinal shortening in normal, acutely ischemic, and scarred myocardium. J Am Soc Echocardiogr 2003;16:415–23.

[19] Yang H, Sun JP, Lever HM, Popovic ZB, Thomas JD, Garcia MJ. Use of strain imaging in detecting segmental dysfunction in patients with hypertrophic cardiomyopathy. J Am Soc Echocardiogr 2003;16:233–9.

[20] Stoylen A, Heimdal A, Bjornstad K, Wiseth R, Skjarpe T. Strain rate imaging ultrasonography in the diagnosis of coronary artery disease. J Am Soc Echocardiogr 2000;13:1053–64.

[21] Ehring T, Heusch G. Left ventricular asynchrony: an indication of regional myocardial dysfunction. Am Heart J 1990;120:1047–57.

[22] Leone BJ, Norris RM, Safwat A, Foex P, Ryder WA. Effects of progressive myocardial ischemia on systolic function, diastolic dysfunction, and load dependent relaxation. Cardiovasc Res 1992;26:422–9.

[23] Nishimura K, Okayama H, Inoue K, Saito M, Yoshii T, Hiasa G, Sumimoto T, Inaba S, Ogimoto A, Funada J, Higaki J. Direct measurement of radial strain in the inner-half layer of the left ventricular wall in hypertensive patients. J Cardiol 2012;59:64–71.

[24] Abraham TP, Nishimura RA. Myocardial strain: can we finally measure contractility? J Am Coll Cardiol 2001;37:731–4.

[25] Urheim S, Edvardsen T, Torp H, Angelsen B, Smiseth OA. Myocardial strain by Doppler echocardiography – validation of a new method to quantify regional myocardial function. Circulation 2000;102:1158–64.